Measuring Harmonics with Inductive Voltage Transformers in Presence of Subharmonics

Measuring Harmonics With Inductive Voltage Transformers in Presence of Subharmonics

Gabriella Crotti, Giovanni D'Avanzo, Palma Sara Letizia, and Mario Luiso, *Member, IEEE*

***Abstract*— The measurement of harmonics is one of the key tasks in modern power systems, performed basically for power quality assessment, verification of planning levels compliance, immunity and compatibility purposes, and so on. Especially at medium voltage (MV) and high voltage (HV) levels, harmonics are always measured through voltage and current transformers (VTs and CTs), which very often are inductive. Recent articles show that inductive VTs and CTs, due to the intrinsic iron core nonlinearity, can introduce errors up to some percent in harmonic measurements. This article aims to investigate in-depth this phenomenon by analyzing how the accuracy of harmonic measurements performed through an inductive MV VT is affected by the presence subharmonics in its input voltage. Subharmonics are spectral components having frequencies lower than the power frequency, that is 50 Hz for European countries. Some theoretical considerations are carried out and the performances of two different inductive MV VTs are tested in various operating conditions. Experimental results show that subharmonics can worsen the harmonic measurements done through inductive VTs up to some tens of percent.**

***Index Terms*— Harmonics, instrument transformer (IT), low-frequency oscillations, power quality (PQ), power system measurements, subharmonics, uncertainty, voltage transformer (VT).**

I. Introduction

THE measurement of harmonics is one of the key tasks in modern power systems, performed basically for power quality (PQ) assessment, verification of planning levels compliance, immunity and compatibility purposes, and so on [1]. In recent years, the presence of harmonics is growing and growing due to the increasing diffusion of switching power converters that serve both for loads as well as for generators, mainly from renewable sources [2].

At medium voltage (MV) and high voltage (HV) levels, harmonics are always measured through voltage and current transformers (VTs and CTs), which very often are of the inductive types. Recent articles [3]–[8] show that inductive VTs and CTs, due to the intrinsic iron core non-linearity, can introduce errors up to some percent in harmonic measurements: this phenomenon has particular relevance for relatively low harmonic frequencies, that is up to some hundreds of hertz.

In this respect, another phenomenon, commonly present in power systems and that could influence the metrological performance of inductive VTs and CTs, is constituted by the subharmonics, which are spectral components having frequencies lower than the power frequency, that is 50 Hz for European countries.

As will be better shown in Section II, subharmonics are due to both distributed energy generation systems, like wind farms, hydropowers, or photovoltaic plants, as well as loads, like arc furnaces and cycloconverters. They have frequencies that range from very low values, down to 0.01 Hz, up to the power frequency. Since the magnetic flux in the core of a transformer is inversely proportional to the frequency of the input signal, the presence of a subharmonic at the input of an inductive instrument transformer (IT) could have a detrimental effect on its performance. To the best of the authors' knowledge, the influence of subharmonics on the metrological performance of an IT is not analyzed in scientific literature nor in international standards.

This article aims at investigating and quantifying the impact of the presence of subharmonic disturbances on the accuracy of harmonic measurements performed through inductive VTs in MV (i.e. $>$ 1 kV) grids.

The activity here described is part of the one developed within the EMPIR 19NRM04 IT4PQ project [9], [10], whose overall scope is to establish measurement methods and procedures for assessing the accuracy of ITs used for PQ measurement.

As a first step, a review of the relevant literature and standards is carried out, to identify realistic variation ranges of subharmonic frequency and amplitude. Then, an extensive experimental analysis is carried out on two commercial inductive VTs, representative of devices commonly used in MV/LV substations. Several experimental tests, varying the harmonic content of input waveforms and other operating conditions, like fundamental amplitude and burden, are performed. They are executed with and without the subharmonic presence, whose frequency and amplitude are chosen in the ranges previously identified. In this way, some general considerations on the degradation of accuracy of harmonic measurement performed through an inductive VT, when also subharmonics are present in the input waveform, are carried out.

This article is organized as follows. Section II gives a thorough review of scientific literature and international standards, dealing with subharmonics, whose outputs are the

Manuscript received May 31, 2021; revised July 16, 2021; accepted August 25, 2021. Date of publication September 24, 2021; date of current version October 12, 2021. This work has received funding from EMPIR 19NRM05 IT4PQ. This project 19NRM05 IT4PQ has received funding from the EMPIR programme co-financed by the Participating States and from the European Union's Horizon 2020 research and innovation programme. The Associate Editor coordinating the review process was Helko E. van den Brom. *(Corresponding author: Mario Luiso.)*

Gabriella Crotti is with the Istituto Nazionale di Ricerca Metrologica (INRIM), 10135 Turin, Italy (e-mail: g.crotti@inrim.it).

Giovanni D'Avanzo and Mario Luiso are with the Department of Engineering, Università degli Studi della Campania "Luigi Vanvitelli", 81031 Aversa (CE), Italy (e-mail: giovanni.davanzo@unicampania.it; mario.luiso@unicampania.it).

Palma Sara Letizia is the the Istituto Nazionale di Ricerca Metrologica (INRIM), 10135 Turin, Italy and also with the Politecnico di Torino, 10129 Turin, Italy (e-mail: p.letizia@inrim.it).

Digital Object Identifier 10.1109/TIM.2021.3111995

variation ranges of subharmonic frequency and amplitude used in the experimental tests. Section III recalls some theoretical considerations, with experimental proof, about the behavior of an inductive VT that help in better understanding the rest of the article. Section IV describes the methodological approach used to test the VTs, the utilized waveforms, and the performance indexes. Section V presents the measurement setup, giving specific focus on the uncertainty budget. Section VI presents the experimental results related to the test of two commercial inductive MV VTs with different specifications, quantifying the degradation of accuracy of harmonic measurement due to the presence of subharmonics. Section VII investigates how different operating conditions, like fundamental amplitude, harmonic amplitude, and burden, can influence the performance of the VTs in presence of subharmonics. Section VIII provides a critical discussion about the obtained results. Finally, Section IX draws the conclusions.

II. Identification of Typical Subharmonic Characteristics

In order to assess how the harmonic measurements performed through inductive VTs are affected by the presence of subharmonic disturbances on the VT input waveform, the first task has been the identification of variation ranges of subharmonic frequency and amplitude typical of actual power systems. Therefore, this section presents a thorough review of literature and standards dealing with subharmonics and, more in general, low-frequency disturbances.

A. Literature Review

The origin of subharmonics is mainly due to energy generation systems and modern loads. Among the distributed energy generation systems, the main contributors to subharmonics injection are wind farms, because of the tower to blade interaction [11], [12], hydropowers, for the long-time constants of their hydraulic components [13]–[16], and photovoltaic plants, especially when they directly supply MV alternating current (ac) bus bars through MV dc/ac (direct current) inverters [17]–[19].

As regards the loads, the subharmonic generation is due to arc furnaces [20], [21], cycloconverters [22]–[24], automated spot-welders, adjustable speed drives, fluctuating motors driving cyclic loads, and power supplies to traction systems [25], [26].

Subharmonics and, more in general, low-frequency oscillations can also occur when there is a mismatch between the generated and demanded power. This power mismatch is caused by quite common events such as the increase of large loads, loss of tie lines, or loss of generating units. As a result, a transient phenomenon characterized by low-frequency oscillations (LFOs) may start [27].

Fig. 1 summarizes the frequency ranges associated with the different subharmonic sources as identified from the performed review. As it can be seen, for disturbances generated by wind farm [11], [12], subharmonics frequencies range from 49 to 0.41 Hz and the most common values are found below 17 Hz. As to the low-frequency disturbances introduced by the hydropower turbines, their frequencies are typically lower than 0.1 Hz and then categorized as ultra-LFOs (ULFOs) [13]–[16]. In particular, ULFOs with frequencies down to 0.01 Hz have been observed in [15].

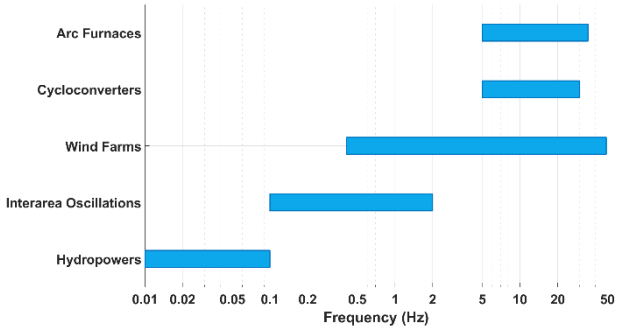

Fig. 1. Typical frequency ranges associated with the different low-frequency disturbances sources.

Both Leonowicz [20] and Garrido-Zafra *et al*. [21] show that subharmonics generated by arc furnaces have frequencies lower than 30 Hz, in particular spectral components having frequencies lower than 10 Hz are appreciable.

In [22], cycloconverters injected subharmonics of 10 Hz with 0.15% amplitude on an MV line whereas in [23] and [24] the cycloconverters produce subharmonics with frequencies from 5 to 35 Hz.

For what concerns the LFOs, their frequency can vary in the 1 to 2 Hz range if they are related to a single generator or in the range 0.1 to 1 Hz if they are associated with a group of generators [27]–[29].

In [30], the results of a measurement campaign focused on subharmonic voltages in an LV distribution system show subharmonic components with a magnitude greater than 1%.

Feola *et al.* [31] aim at assessing the performances of phase-locked loop systems (PLL) in the presence of some power grid disturbances; among them, they have assumed subharmonics from 0 Hz up to the power frequency with a fixed amplitude of 1%. In [32], among the possible grid disturbances, a subharmonic of 1 Hz and 10% is assumed.

In [33] the impact of subharmonics on a single-phase transformer is studied. To perform this analysis, the authors considered subharmonics with 0.9% fixed amplitude and frequency variable from 1 to 10 Hz.

B. Standards Review

Some additional indications, related to typical ranges of variations of subharmonic amplitude and frequency, are provided by the standards.

It is worth noting that both the IEEE standards [34], [35] and IEC standards [36]–[38], refer to the subharmonics as interharmonics since they define the latter as "voltages or currents having frequency that is not an integer multiple of the frequency at which the supply system is designed to operate."

In [34], for systems with rated voltage from 1 up to 69 kV, the limit set for the interharmonics with frequency lower than 25 Hz is equal to 3%. In [35], a typical voltage magnitude below 2% is assumed for the interharmonics with frequency

TABLE I
SUBHARMONIC TEST PARAMETERS

Test group	Frequency (Hz)	Amplitude (% of fund)
I	0.01 – 0.02 – 0.05	0.1
II	0.1 – 0.2 – 0.5	0.1 – 0.3
III	1 – 2 – 5 – 10 – 20	0.1 – 1 – 3

from 0 Hz to 9 kHz. Another low-frequency disturbance, presented in [35], is the voltage fluctuation and it is described as a phenomenon having spectral content at frequencies lower than 25 Hz and typical magnitude in the 0.1% to 7% range.

Standards [36] and [38] discuss possible LV and MV sources of interharmonics and subharmonics. As output, in [36] it is stated that discrete frequencies in the range of 0 Hz to 2500 Hz can be found in the grid and their possible amplitudes are 0.5% or even more.

In [37], a conservative planning level for interharmonics in MV grids is set to 0.2%.

C. Identified Parameters of Subharmonic Disturbances

As a general consideration, literature analysis highlights that subharmonics are strictly connected to renewable energy sources and, therefore, they have to be considered as a growing issue of the power grid.

The analysis of literature and standards can be summarized as follows:

1) Subharmonic frequencies can range from values very close to the power frequency (49 Hz) down to approaching 0 Hz level (ULFO case). However, the most common values of the subharmonic frequencies are lower than 20 Hz;
2) Subharmonic amplitudes are often lower than 1% but the standards take into account also higher magnitude levels (e.g., 3% for MV grids in [34]).

Based on these considerations, the experimental analysis described in Sections IV, VI, and VII is carried out considering the test parameters given in Table I, where subharmonics are grouped based on common amplitude levels.

III. VT NONLINEAR BEHAVIOR: BACKGROUND CONSIDERATIONS

According to Faraday's law [39], when a transformer is working in no-load conditions and is supplied with a sinusoidal voltage source on the primary winding, it produces a sinusoidal flux. The amplitude of the flux is directly proportional to the applied voltage and inversely proportional to the frequency. To sustain the flux, a magnetizing current is generated in the primary winding. The magnetizing current is related to the flux via the magnetization characteristic [40] of the transformer ferromagnetic core.

Fig. 2 shows the magnetizing current of a commercial inductive MV VT when a sinusoidal voltage source is applied to the primary winding. Due to the nonlinearity of the ferromagnetic core, the magnetizing current is far from sinusoidal.

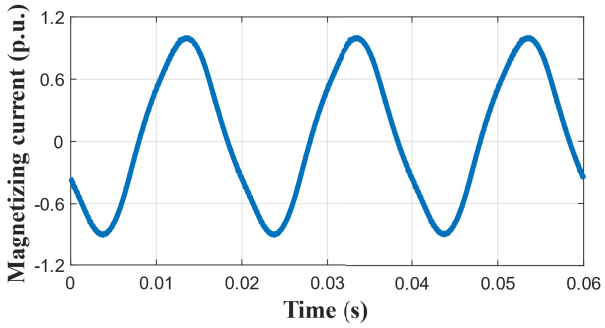

Fig. 2. Magnetizing current wave shape of a commercial inductive MV VT when a sinusoidal voltage is applied to the primary winding.

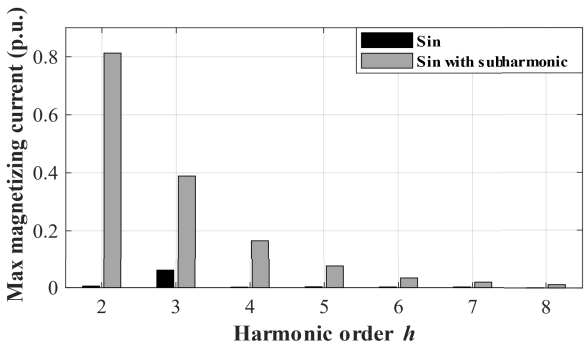

Fig. 3. Harmonics of magnetizing current given in p.u. of fundamental component without subharmonic (left) and with a subharmonic (right) with amplitude of 0.1% and frequency of 0.01 Hz.

In fact, as it can be seen from Fig. 3 (left), the spectrum of the magnetizing current shown in Fig. 2, includes harmonic distortion even when a rated sinusoidal voltage at rated frequency is applied to the primary winding, especially the third harmonic (0.05% of the fundamental). As a result, also the secondary voltage presents spurious harmonic tones.

In literature [3]–[6], some articles deal with techniques for the characterization and compensation of this undesirable effect. As Section IV-A briefly recalls, some authors have shown that it is possible to compensate for the spurious harmonics, produced in the output voltage, by characterizing the VT using a sinusoidal primary voltage [3].

If a low-frequency sinusoidal voltage is superimposed to the rated voltage at the fundamental frequency, the total flux is the sum of two components: the first component is given by the fundamental tone and the second is given by the low-frequency voltage [33]. In this condition, a higher flux must be sustained by a higher magnetizing current; therefore, its spectral components are amplified as can be seen from Fig. 3 (right). As a result, the voltage at the secondary winding is more distorted. Furthermore, the low-frequency oscillation of the primary voltage generates an oscillation of the total flux. For this reason, the magnetization curve changes with a periodicity given by the parameters of the low-frequency component, and the harmonic components of the magnetizing current are not constant in time. In fact, as it can be seen in Fig. 4 when a low-frequency voltage is superimposed on the fundamental component, the measured amplitude of the

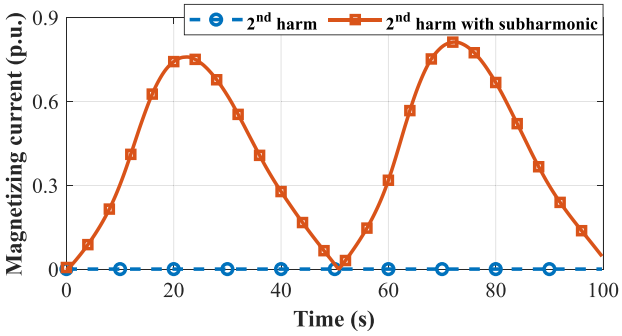

Fig. 4. Amplitude of second harmonics of magnetizing current given in p.u. of fundamental component without 0.01 Hz subharmonic (circle markers) and with subharmonic (square markers).

second harmonic of the magnetizing current oscillates, while it is constant in time in the sinusoidal case (even if it has very low amplitude, about 0.01%); the oscillation frequency is twice the subharmonic frequency.

So, let us imagine that a VT is supplied a waveform composed of the fundamental tone, harmonic components, and subharmonic tones, due, f.i., to the phenomena described in Section II. Considering what has been here discussed, the harmonic components of the secondary voltage are the result of the vector sum of: 1) the actual harmonics superimposed on the primary voltage (modified by the systematic VT ratio and phase errors at the specific harmonic frequency) and 2) the spurious harmonic components due to both the fundamental and the low-frequency components.

IV. Test Description

This section describes the tests carried out to analyze how the accuracy of harmonic measurements performed through inductive VTs is affected by the presence of subharmonics in the input voltage, as well as the indexes used to quantify this impact. All the tests are performed in three steps.

A. Sinusoidal Test and SINDICOMP

The VTs are preliminarily characterized with sinusoidal input, varying the amplitude in the range from 80% to 120%, and having fixed rated frequency. This test is required for the application of the SINDICOMP technique. In fact, since the scope is to quantify the impact of subharmonics on the measurement of harmonics, the contribution of the fundamental tone to harmonic ratio and phase errors should be attenuated. Therefore, the spurious harmonic tones measured in this step are removed from the harmonic components measured also in the second and third steps, described, respectively, in Section IV-B and Section IV-C.

For sake of clarity, here the SINDICOMP technique is briefly recalled, whereas a thorough description can be found in [3]. As shown in Section III, due to the iron-core non-linearity, if a VT is supplied with a sinusoidal input, the secondary voltage is distorted, because of the spurious harmonic components of the magnetization current. Thus, according to [3], a primary voltage phasor at each harmonic h can be expressed as

$$\bar{V}^{d}_{p,h} = \bar{V}^{d}_{s,h} - \bar{V}^{\sin}_{s,h} \tag{1}$$

where

1) The subscripts "p" and "s" stand for primary and secondary side, respectively;
2) The superscripts "d" and "sin" refer to tests performed under distorted and sinusoidal conditions;
3) The subscript h stands for h-order harmonic;
4) The secondary quantities are here referred to the primary side of the VT, so that the transformation ratio does not explicitly appear (that is the quantities at the secondary side are multiplied by the rated ratio of the VT);

The secondary voltage harmonic components (amplitude and phase of $\bar{V}^{\sin}_{s,h}$), measured under sinusoidal conditions, can then be used as a correction for the spurious harmonic tones produced in the output voltage due to the iron core non-linearity and the presence of the fundamental tone. By applying the compensation illustrated in (1), the non-linearity errors are strongly reduced and, therefore, the VT behavior can be considered linear [3].

B. Reference Test: FH1

In the second step, the VT is supplied with waveforms composed by the fundamental component, at rated amplitude and frequency, and one harmonic component with amplitude equal to 1% of the fundamental and harmonic order h varying from the second up to tenth (Fundamental plus one Harmonic, FH1 test). Harmonic ratio and phase errors are evaluated through the following equations:

$$\varepsilon_h = \frac{k_r V_{s,h} - V_{p,h}}{V_{p,h}} \tag{2}$$

$$\varphi_h = \varphi_{s,h} - \varphi_{p,h} \tag{3}$$

where

1) $k_r = V_{p,r}/V_{s,r}$ is the rated transformation ratio ($V_{p,r}$ and $V_{s,r}$ are the rated primary and secondary voltages);
2) $V_{p,h}$ and $V_{s,h}$ are the root mean square (rms) values of the primary and secondary h-order harmonic voltage;
3) $\varphi_{p,h}$ and $\varphi_{s,h}$ are the phase angles of the primary and secondary h-order harmonic voltage.

C. Subharmonic Test: FHS

In the third step, a subharmonic voltage is superimposed on the FH1 waveforms described in Section IV-B. This is called the fundamental plus one harmonic and one subharmonic (FHS) test. The frequency and amplitude of subharmonic components are chosen according to Table I.

The FHS test waveform is composed by: 1) a fundamental component, having rated amplitude and frequency; 2) a harmonic component with amplitude equal to 1% of the fundamental tone amplitude and order variable from the second to tenth; 3) a subharmonic tone from one of the test group shown in Table I. All the combinations frequency-amplitude of Table I groups are considered in the experimental tests.

The ratio (ε_h) and phase (φ_h) errors at the h-order harmonic are evaluated according to (2) and (3), respectively. The evaluation is performed over an integer number of periods

TABLE II
RATED CHARACTERISTICS OF THE ANALYZED VTs

	Rated primary voltage (kV)	Rated secondary voltage (V)	Rated burden (VA)	Accuracy class
VTA	$20/\sqrt{3}$	$100/\sqrt{3}$	30	0.5
VTB	$11/\sqrt{3}$	$110/\sqrt{3}$	50	0.5

of the FHS signal in non-overlapped 200 ms time frames, according to [41] for a 50 Hz power system.

D. Quantification of Subharmonic Impact

To quantify the effect of the subharmonic voltage on the harmonic ratio and phase errors evaluated according to (2) and (3), respectively, the following indices are used:

$$\xi_h = \max_{\cup w_n} |\varepsilon_h - \overline{\varepsilon_h}| \tag{4}$$

$$\psi_h = \max_{\cup w_n} |\varphi_h - \overline{\varphi_h}| \tag{5}$$

where

1) $\cup w_n$ is the union of time frames in which ratio and phase errors are evaluated. For every considered subharmonic, $\cup w_n$ is always equal to an integer multiple of the period of the subharmonic. Each w_n equals ten cycles of fundamental frequency;
2) ε_h (φ_h) is the ratio (phase) error at h-order harmonic, evaluated in the different time frames w_n;
3) $\overline{\varepsilon_h}$ ($\overline{\varphi_h}$) is the mean value of ratio (phase) errors at h-order harmonic, which equals the ratio (phase) error evaluated over a time interval that represents an integer multiple of the period of the subharmonic.

In practice, ξ_h (ψ_h) evaluates the maximum absolute increment of the harmonic ratio (phase) error caused by the presence of the subharmonic.

V. MEASUREMENT SETUP

A. Measurement Setup Description

The analyzed VTs are two commercial resin insulated VTs for MV phase to ground measurement applications. The VTs' main features are summarized in Table II.

The VT characterization is carried out with the measurement setup [42] shown in Fig. 5. The voltage signals are generated by the Arbitrary Waveform Generator (AWG) National Instrument (NI) PCI eXtension for Instrumentation (PXI) 5421, with 16 bit, variable output gain, ±12 V output range, 100 MHz maximum sampling rate, 256 MB of onboard memory. The AWG is inserted in a PXI chassis and the 10 MHz PXI clock is used as a reference clock for its PLL circuitry. Another AWG is used to generate a 12.8 MHz clock, which is used as a time base clock for the acquisition system.

The low voltage waveform generated by the AWG is amplified by a Trek high-voltage power amplifier (±30 kV, ±20 mA, 20 kHz). The applied MV voltage values are scaled by a reference resistive-capacitive voltage divider (RCVD) designed, built, and characterized at INRIM [43], [44]. The reference RCVD has a rated primary voltage equal to 30 kV

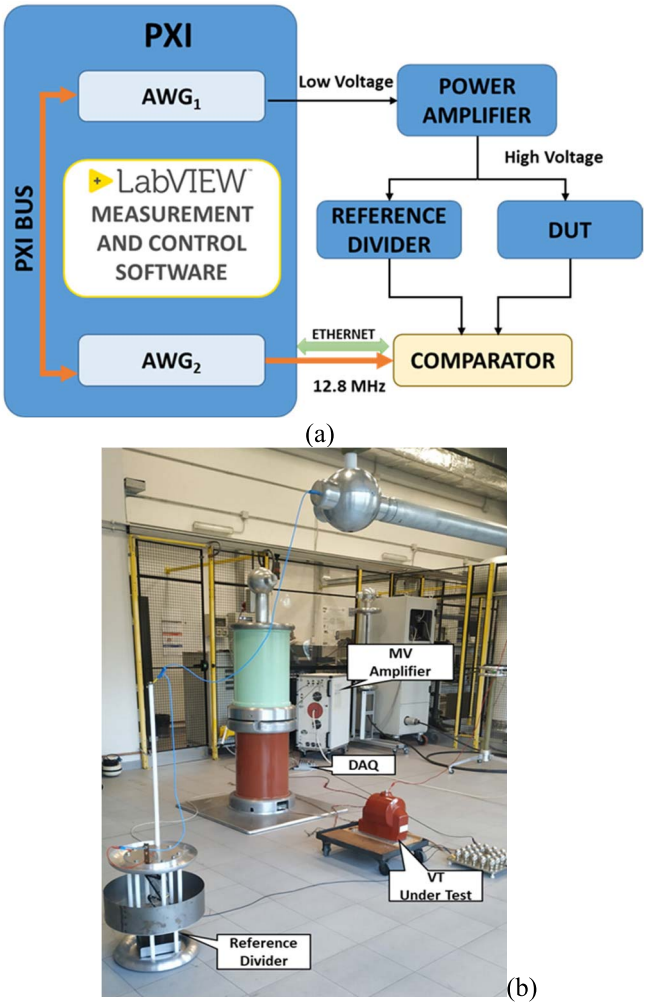

Fig. 5. Setup for the VT characterization. (a) Block diagram and (b) generation and measurement circuit at Italian National Metrology Institute (INRIM).

(peak value) and it is designed to have a flat frequency response from 0 Hz to 12 kHz. The RCVD high voltage arm is composed of four bipoles series connected with a zig-zag path. In particular, each bipole is composed of the parallel connection of a 30 MΩ resistor and a 300 pF capacitor. The low voltage harm includes a 12 kΩ resistor parallel connected to a 750 nF capacitor. As the RCVD insulation, it is air-insulated and not resin-immersed. Consequently, since there are no dielectric nor ferromagnetic components, it can be considered a linear device.

The acquisition system is composed of a NI compact Data AcQuisition system (cDAQ) chassis with various input modules having 24 bit resolution, 50 kHz maximum sampling rate, and input range from ±500 mV up to ±425 V. Since generation and acquisition are synchronized, the discrete Fourier transform (DFT) of the acquired samples is used to evaluate the voltage fundamental and harmonic phasors.

B. Measurement Setup Uncertainty Budget

Different procedures are used to evaluate the uncertainty of the measurement setup at power frequency and at harmonic frequencies.

TABLE III
RATIO ERROR UNCERTAINTY CONTRIBUTIONS FROM 5 TO 20 kV AND FROM 100 Hz UP TO 1 kHz

Uncertainty Source	Standard Uncertainty (μV/V)
RCVD Calibration	30
Amplitude Dependence	40
Frequency response	35
Proximity effect	21
Stability	10
Acquisition system	30
Relative expanded uncertainty (Level of confidence 95%): **144 μV/V**	

TABLE IV
PHASE ERROR UNCERTAINTY CONTRIBUTIONS FROM 5 kV TO 20 kV AND FROM 100 Hz UP TO 1 kHz

Uncertainty Source	Standard Uncertainty (μrad)
RCVD Calibration	30
Amplitude Dependence	16
Frequency response	140
Proximity effect	9
Stability	1
Acquisition system	30
Relative expanded uncertainty (Level of confidence 95%): **295 μrad**	

The uncertainty (level of confidence 95%) of the measurement setup at power frequency is 70 μV/V and 70 μrad and it is obtained by comparison with an INRIM standard VT.

A detailed description of the procedures used to characterize the systematic ratio and phase errors, and the related uncertainty budgets, of the measurement setup at harmonic frequencies, as in (2) and (3), can be found in [43]. In particular, the reference divider has been characterized by carrying out various sets of tests which include: 1) evaluation of the voltage dependence of the divider scale factor (SF), defined as the ratio of the applied to the output voltage; 2) measurement of the frequency response at reduced amplitude (300 V); and 3) stability and 4) proximity tests performed at rated frequency. Instead, amplitude and frequency calibration of the acquisition modules is performed using a Fluke 5730A calibrator (dc up to 1.2 MHz, up to 1100 V) as a reference system.

The uncertainty budgets from 100 Hz up to 1 kHz for the ratio and phase errors are detailed and quantified in Tables III and IV, respectively.

VI. EXPERIMENTAL EVALUATION OF SUBHARMONIC IMPACT

In this section, the results of the tests performed for assessing the subharmonic influence on VT_A and VT_B performance are presented. In particular, in Section V-A, the errors introduced by VT_A and VT_B in fundamental and harmonic measurement, without the subharmonic influence, are provided. In Section V-B the subharmonic effects on VT_A and VT_B performance are given. All the results shown in the following have been compensated through the SINDICOMP technique (first step), as explained in Section IV-A.

A. Reference Tests: FH1

In this section, the results obtained from the VTs characterization under FH1 (see Section IV-B) waveforms are reported. The errors ξ_h and ψ_h evaluated in this step can be assumed as the reference condition to quantify the additional contributions introduced by the subharmonic presence. Null burden condition is assumed.

The results of the FH1 tests performed on VT_A and VT_B are shown in Table V. For both the VTs, after applying the SINDICOMP technique, ξ_h and ψ_h are comparable to the measurement uncertainties and in the order of, respectively, 0.02% and 0.02 crad.

B. Impact of Subharmonics on Harmonic Measurements

This section presents the results of the FHS test (see Section IV-C) performed on VT_A and VT_B to assess their performance in fundamental and harmonic measurement in presence of a subharmonic component.

The VTs were tested in null burden conditions. Section VII will show the impact of different choices for fundamental amplitude, harmonic amplitude, and burden.

As anticipated in Section III, the presence of a subharmonic component in the VT input voltage produces spurious harmonic phasors in the VT secondary voltage. These harmonic phasors, evaluated over non-overlapping observation intervals ω_n, each one 200 ms long according to [41] for a 50 Hz power system, have a periodic behavior and thus cause time-varying ratio and phase errors at the considered harmonic frequency. An experimental example is given in Fig. 6 where the time behavior of the VT_A second harmonic ratio error, in presence of a 0.1%, 0.01 Hz subharmonic is shown. To better evaluate the impact of the subharmonic, the time behavior of the second harmonic ratio error measured under the FH1 test is also reported in Fig. 6. The oscillation characteristics are strongly related to the subharmonic parameters. In particular, the oscillation period is equal to the subharmonic period whereas the oscillation amplitude depends on both the subharmonic amplitude as well as the frequency.

A comprehensive overview of the VT_A and VT_B behaviors is provided in figures from Fig. 7–16 where the maximum absolute increments of ratio and phase errors (ξ_h, ψ_h) in the various test conditions are shown.

In particular, Figs. 7 and 8 show the results related to the VT_A and VT_B performance in fundamental tone measurement.

In this case, the test waveform is composed of fundamental components having rated amplitude and frequency, a subharmonic component with amplitude and frequency according to Table I, and no harmonic tones.

The subharmonic presence has a low impact on the measurement of the fundamental tone for both the VTs under test being in some cases lower than the measurement uncertainty. For VT_A, the maximum values of ξ_1 and ψ_1 are equal to 0.05% and

TABLE V
MAXIMUM ABSOLUTE RATIO AND PHASE ERROR VARIATIONS OF VTs UNDER TEST WITHOUT SUBHARMONICS

	Harmonic order									
	1	2	3	4	5	6	7	8	9	10
					VT_A					
ξ_h(%)	0.0002	0.02	0.02	0.02	0.01	0.01	0.01	0.01	0.01	0.01
ψ_h(crad)	0.0002	0.02	0.02	0.02	0.02	0.02	0.01	0.01	0.02	0.02
					VT_B					
ξ_h(%)	0.0003	0.05	0.03	0.02	0.03	0.03	0.02	0.02	0.02	0.03
ψ_h(crad)	0.0002	0.04	0.03	0.02	0.02	0.02	0.02	0.02	0.03	0.02

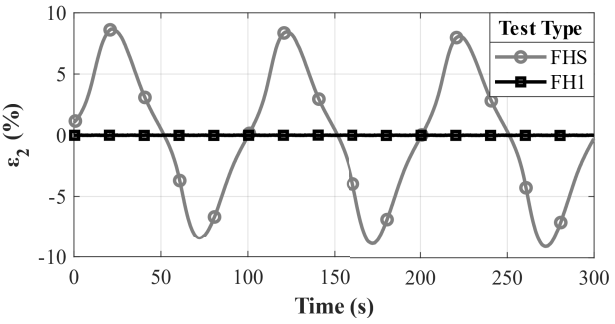

Fig. 6. Ratio errors of VT_A at second harmonic with (circle markers) and without (square marker) subharmonic component at 0.01 Hz and 0.1%.

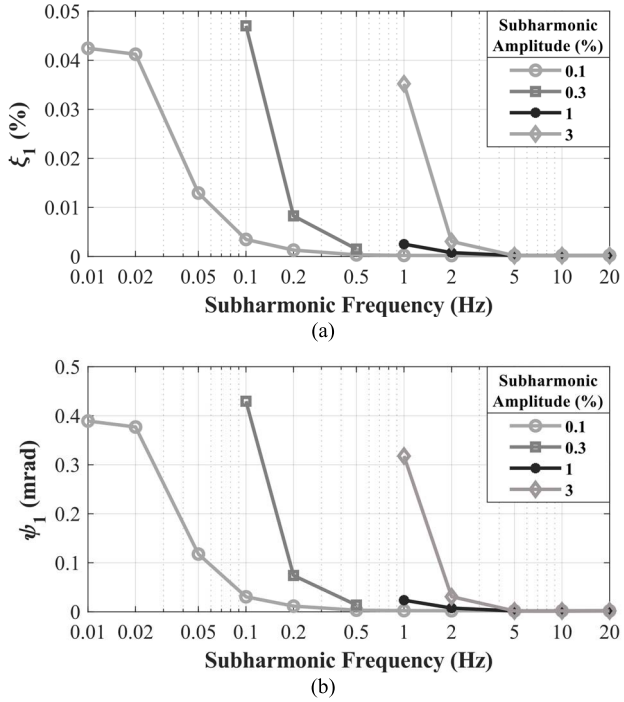

Fig. 7. Maximum absolute increments of VT_A (a) ratio errors and (b) phase errors at fundamental frequency, in presence of subharmonics with various amplitudes and frequencies.

0.40 mrad and they are observed in presence of a 0.3%, 0.1 Hz subharmonic. For VT_B, instead, the maximum values of ξ_1 and ψ_1 are close to 0.05% and 0.41 mrad and are found in presence

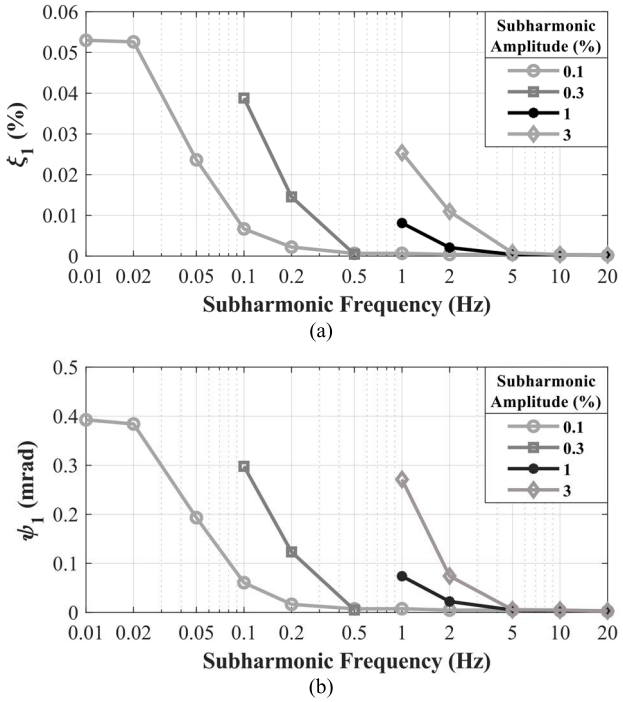

Fig. 8. Maximum absolute increments of VT_B (a) ratio errors and (b) phase errors at fundamental frequency, in presence of subharmonics with various amplitudes and frequencies.

of a 0.1% and 0.01 Hz subharmonic. In practice, the measured increments represent a small fraction of the 0.5 accuracy class (the accuracy class of the analyzed VTs) limits of an IT, which are 0.5% and 9 mrad respectively for ratio and phase errors. Thus, even in presence of subharmonics, an MV VT remains compliant with its accuracy class limits as regards the fundamental tone measurements.

From Figs. 9–16, the maximum absolute error increments (ξ_h, ψ_h) are shown for each generated harmonic, each subharmonic frequency, and for a fixed subharmonic amplitude. It is worth noting that for all these figures, a logarithmic scale has been chosen for the y-axes, since the error increments extend over a wide range of values.

Looking at all the figures from Figs. 9–16, it is evident that, regardless of subharmonic parameters, the most affected harmonics are the firsts, in particular, the second and the third

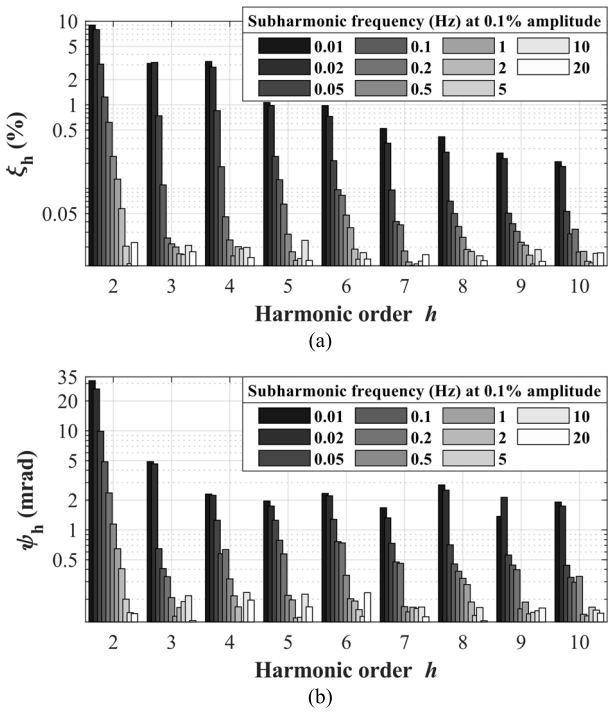

Fig. 9. Maximum absolute increments of VT_A (a) ratio errors and (b) phase errors at harmonic order h, in presence of subharmonics with 0.1% amplitude and various frequencies.

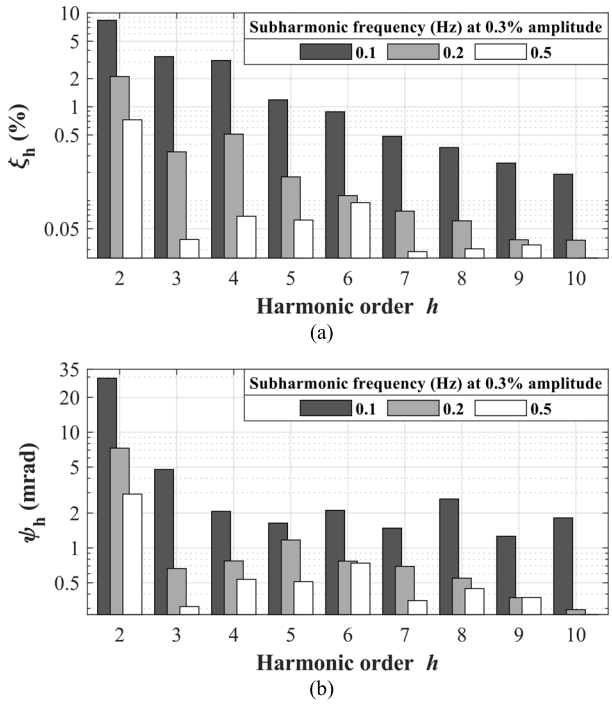

Fig. 10. Maximum absolute increments of VT_A (a) ratio errors and (b) phase errors at harmonic order h, in presence of subharmonics with 0.3% amplitude and various frequencies.

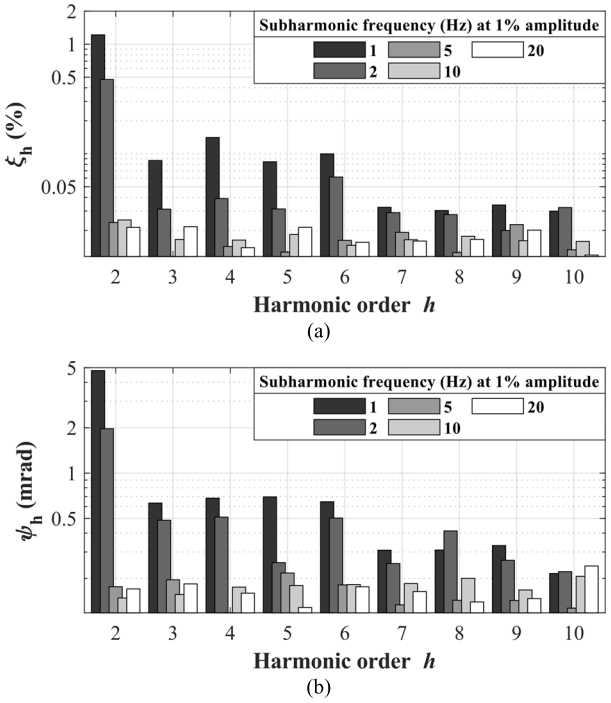

Fig. 11. Maximum absolute increments of VT_A (a) ratio errors and (b) phase errors at harmonic order h, in presence of subharmonics with 1% amplitude and various frequencies.

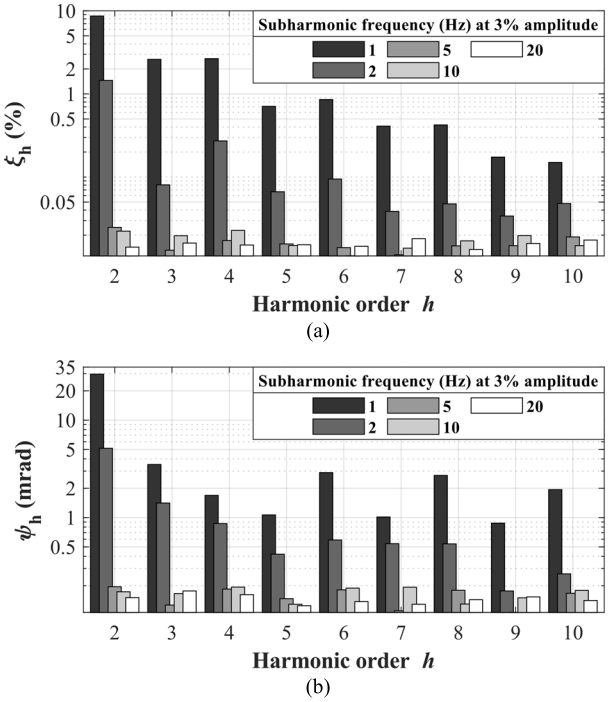

Fig. 12. Maximum absolute increments of VT_A (a) ratio errors and (b) phase errors at harmonic order h, in presence of subharmonics with 3% amplitude and various frequencies.

harmonics. This result is consistent with the analysis done in Section III (see Fig. 3). As a general consideration, analyzing the single h harmonic, it can be observed that ξ_h and ψ_h increase with a monotonous behavior when the subharmonic frequency decreases.

Looking at any single harmonic in Fig. 9 (VT_A) and Fig. 13 (VT_B), it can be observed that the maximum error increments

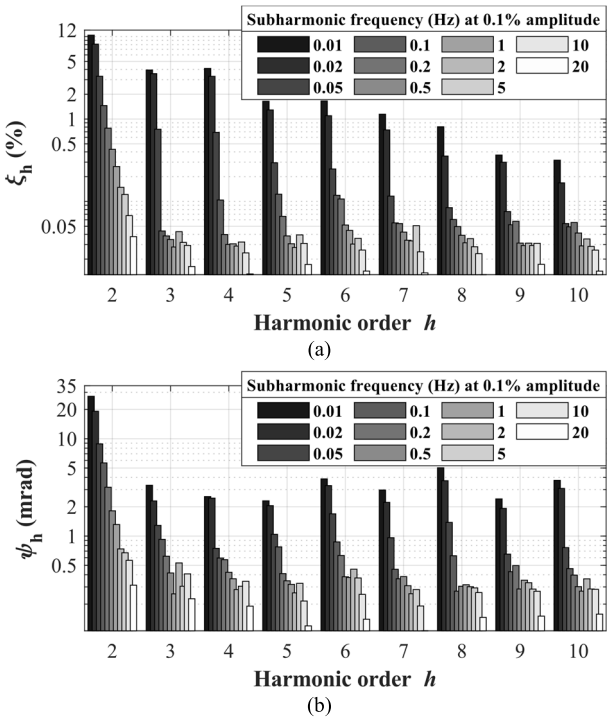

Fig. 13. Maximum absolute increments of VT_B (a) ratio errors and (b) phase errors at harmonic order h, in presence of subharmonics with 0.1% amplitude and various frequencies.

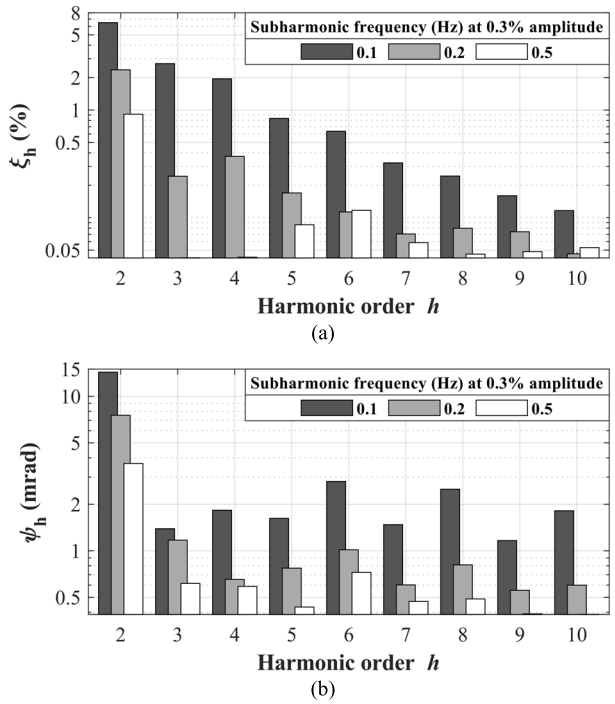

Fig. 14. Maximum absolute increments of VT_B (a) ratio errors and (b) phase errors at harmonic order h in presence of subharmonics with 0.3% amplitude and various frequencies.

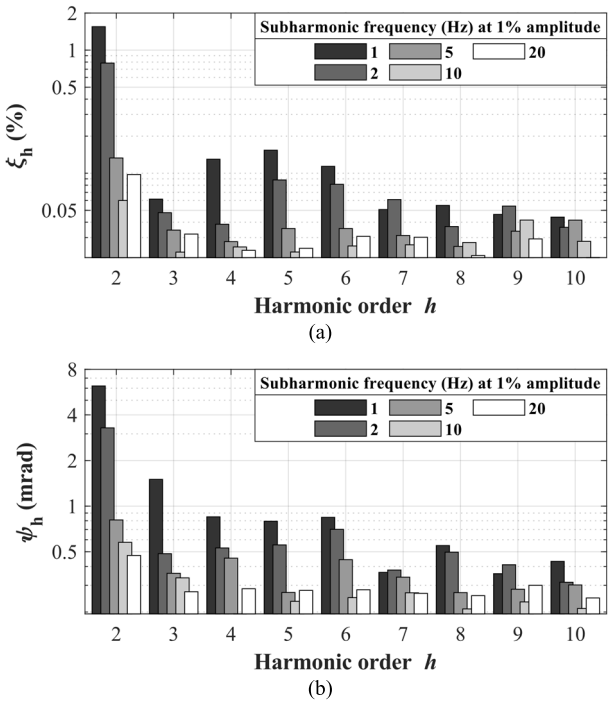

Fig. 15. Maximum absolute increments of VT_B (a) ratio errors and (b) phase errors at harmonic order h, in presence of subharmonics with 1% amplitude and various frequencies.

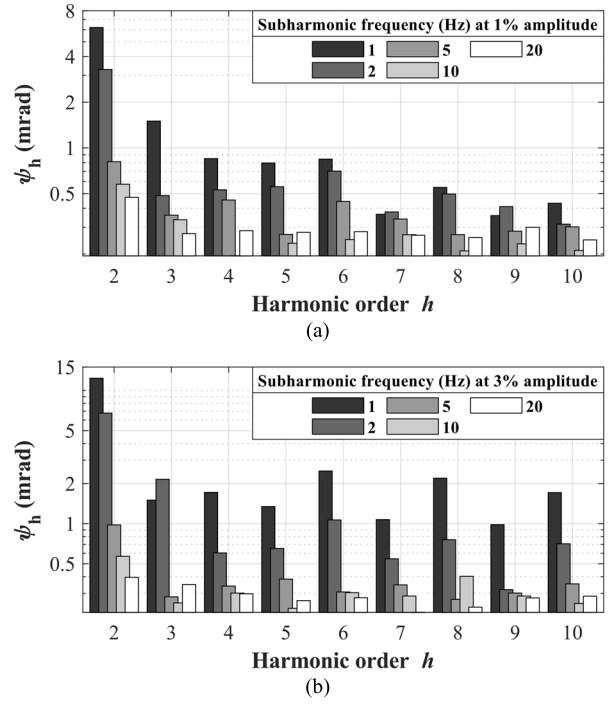

Fig. 16. Maximum absolute increments of VT_B (a) ratio errors and (b) phase errors at harmonic order h, in presence of subharmonics with 3% amplitude and various frequencies.

caused by the presence of a 0.1% subharmonic vary up to two orders of magnitude, depending on the subharmonic frequency. More in particular, considering the VT_A results (Fig. 9), ξ_2 and ψ_2 in presence of a 0.1%, 0.01 Hz subharmonic are equal to 9.00% and 32.05 mrad, whereas they significantly decrease to 0.02% and 0.14 mrad if a 0.1% but 20 Hz subharmonic is

considered. For VT_B, the 0.1%, 0.01 Hz subharmonic makes ξ_2 and ψ_2 equal to 10.42% and 27.28 mrad; these values decrease to 0.04% and 0.31 mrad when the effect of a 0.1%, 20 Hz subharmonic is evaluated.

As regards the subharmonic amplitude effect, higher values of ξ_h and ψ_h are found for a higher value of subharmonic amplitudes. In order to prove this consideration, let us consider the case of 1 Hz subharmonic with three different amplitudes, equal to 0.1% (Fig. 9 for VT_A and Fig. 13 for VT_B), 1% (Fig. 11 for VT_A and Fig. 13 for VT_B), and 3% (Fig. 12 for VT_A and Fig. 16 for VT_B), and let us analyze ξ_2 and ψ_2, i.e. at the second harmonic. For VT_A, with the increase of subharmonic amplitude from 0.1% to 1% and 3%, ξ_2 increases from 0.13% to 1.22% and 8.70%, respectively, whereas ψ_2 increases from 0.65 mrad to 4.80 mrad and 29.65 mrad, respectively.

For VT_B, instead, ξ_2 increases from 0.26% to 1.55% and 4.80%, respectively, whereas ψ_2 increases from 1.31 mrad to 6.21 and 12.36 mrad, respectively.

VII. Impact of Operating Conditions

To quantify the subharmonic impact on the VT performance when it is used under operating conditions different from those assumed in the previous section, three different test quantities are considered in the following: 1) the amplitude of the fundamental component; 2) the amplitude of the harmonic tone; and 3) the burden condition.

The subharmonic chosen for these additional analyses is the one that, according to the results shown in Section VI, most influenced the performance of the VTs, i.e., the subharmonic characterized by 0.1% amplitude and 0.01 Hz frequency.

For sake of brevity, the analyses here shown refer only to the ratio error of VT_A in harmonic measurement. Similar considerations can be done for VT_B and are also valid for phase error.

A. Fundamental Tone Amplitude

With respect to the analysis carried out in Section VI by considering the rated value for the fundamental component, other two fundamental tone amplitudes are considered here: 80% and 120% of the rated primary voltage. The harmonic component superimposed on the fundamental tone has an amplitude equal to the 1% of the fundamental tone and order variable from the second to the tenth. Tests are carried out with a null burden.

Results are shown in Fig. 17. For all the harmonic orders, ξ_h increases with the increase of the fundamental tone amplitude. When the fundamental tone is 80% of the rated value, the subharmonic influence leads to a ξ_2 equal to 5.48%, whereas the same quantity reaches 12.66% if the fundamental tone amplitude increases to 120% of the rated one.

Consequently, the VT full operating range, that is from 80% to 120% [45], has to be accounted for in the analysis, since the evaluated maximum error increments due to the subharmonic presence can vary up to an order of magnitude.

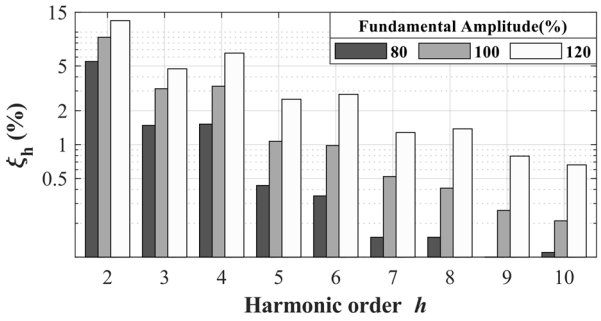

Fig. 17. Maximum absolute increments of VT_A ratio errors at harmonic order h, with various values of fundamental amplitude, in presence of a 0.1%, 0.01 Hz subharmonic component.

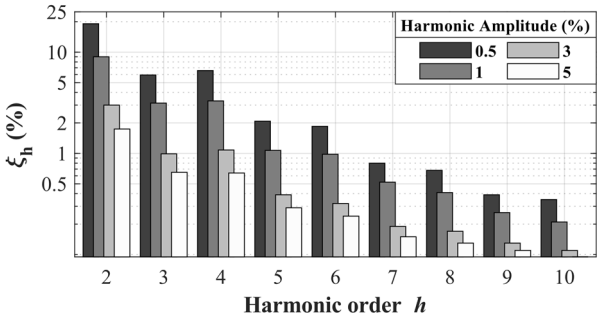

Fig. 18. Maximum absolute increments of VT_A ratio errors at harmonic order h, with various values of harmonic amplitude, in presence of a 0.1%, 0.01 Hz subharmonic component.

B. Harmonic Amplitude

This section aims at assessing the impact of the subharmonic presence on the VT when it is used to measure harmonics having different amplitude levels. For this purpose, FHS tests with three additional harmonic amplitudes are performed: 0.5%, 3%, and 5% of the fundamental tone. The other test parameters and operating conditions are those assumed in Section VI.

Results are shown in Fig. 18, where also the maximum ratio errors increment at 1% harmonic amplitude case is reported.

Looking at Fig. 18, it can be observed that the ratio error maximum increments significantly increase for low values of harmonic amplitude. This is due to the fact that when the amplitude of the harmonic tone injected at the primary side is low, it is comparable to the amplitude of the correspondent spurious harmonic introduced at the secondary side by the presence of the subharmonic.

Moreover, it can be observed that, especially for the first harmonics, the maximum error increments are inversely proportional to the amplitude of the injected harmonic. For instance, ξ_4 (i.e. the maximum ratio error increment at the fourth harmonic) doubles from 3.30% to 6.58% when the harmonic amplitude is halved from 1% to 0.5% and it is reduced to one fifth, from 3.30% to 0.63%, when the harmonic amplitude increases from 1% to 5%.

C. Burden Condition

The scope of this section is to quantify the impact of the subharmonic on VT performance when it is used at

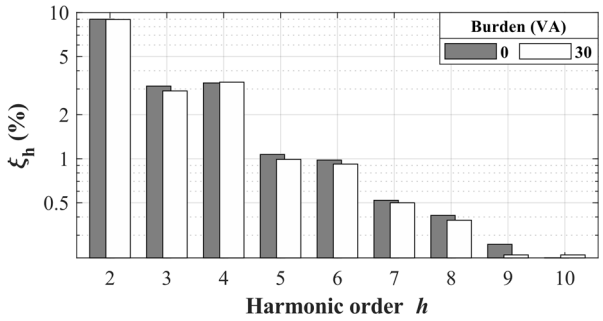

Fig. 19. Maximum absolute increments of VT_A ratio errors at harmonic order h, with null and rated burden (30 VA), in presence of a 0.1%, 0.01 Hz subharmonic component.

the rated burden condition. For this purpose, VT_A has been characterized under its rated burden condition, i.e., using a 30 VA ohmic-inductive burden with a $\cos(\varphi) = 0.8$ active factor. The fundamental tone has rated amplitude and frequency. The harmonic component superimposed on the fundamental tone has an amplitude equal to the 1% of the fundamental tone and order variable from the second to the tenth.

Fig. 19 shows that the burden condition does not represent a significant influence parameter since the results measured under the two different conditions are very similar. In particular, the maximum difference between the tests performed with zero burden and rated burden is found at the third harmonic where the two errors differ by 0.23%, whereas for the other harmonics, this difference is below 0.1%.

VIII. Discussion of the Results

From the analysis of the results shown in Sections VI and VII, some general considerations about how the accuracy of harmonic measurements performed through inductive VTs are affected by the presence of subharmonics in the input voltage can be carried out.

The fundamental tone measurement is practically not affected by the presence of subharmonics, since the maximum measured ratio and phase error increments are about 0.05% and 0.4 mrad, which are a small fraction of the limits of the 0.5 accuracy class for a VT (0.5% and 9 mrad), that is the accuracy class of the analyzed VTs. Moreover, in most cases, the fundamental maximum absolute increments are comparable with the measurement uncertainties.

In presence of subharmonic, harmonic ratio and phase errors increase when the subharmonic amplitude increase and when the subharmonic frequency decreases.

The harmonic measurements are highly affected by the presence of a subharmonic, especially the second and the third harmonics, where ratio and phase errors can increase up to values as high as 20% and 30 mrad.

However, the presence of a subharmonic in the input voltage does not represent always a critical situation for the performance of an inductive VT at harmonic frequencies.

In fact, the harmonic maximum absolute increments for VT_A are comparable with the measurement uncertainty when the subharmonic has: 1) frequency higher than 5 Hz and amplitude up to 3% or 2) amplitude up to 1% and frequency higher than 1 Hz.

The harmonic maximum absolute increments for VT_B are higher than those observed for VT_A. Only in few cases, the increments related to 10- and 20-Hz subharmonic frequency, are comparable with measurement uncertainty.

For both $VT_A$and VT_B, the 0.5 accuracy class limits are exceeded with subharmonics characterized by:

1) 0.1% amplitude and frequency from 0.01 Hz to 0.2 Hz (ULFOs and LFOs cases);
2) 0.3% amplitude and frequency up to 0.5 Hz;
3) 1% amplitude and frequency up to 1 Hz;
4) 3% amplitude and frequency up to 2 Hz;

The study of the impact of operating conditions in terms of fundamental and harmonic amplitude represents a necessary step for this analysis. In fact, the harmonic absolute maximum error significantly increases as the fundamental amplitude increases and decreases when the amplitude of the harmonics increases. On the contrary, in presence of a subharmonic, the burden condition does not significantly alter the performance.

IX. Conclusion

This article has presented that the accuracy of harmonic measurement performed through inductive MV VTs can be affected by the presence of subharmonics in the input voltage.

Appropriate variation ranges for subharmonic amplitude and frequency were retrieved from a thorough review of literature and standards. Then, they are used in an extensive experimental activity performed on two commercial inductive MV VTs, representative of devices commonly installed in MV/LV substations.

The main outcomes of this article can be summarized as follows:

1) In presence of subharmonics, the errors introduced by an inductive VT in the measurement of harmonics can be much higher than the case in which they are not present;
2) In presence of subharmonics, the harmonic ratio and phase errors have no constant values over time, they oscillate and, therefore, they cannot be easily compensated;
3) The harmonic ratio and phase errors of an inductive VT, in presence of subharmonics, can reach values as high as 20% and 30 mrad, far exceeding the limit of its accuracy class, especially for ratio error;
4) Harmonic ratio and phase errors increase both when the subharmonic amplitude increases as well as when the subharmonic frequency decreases;
5) Particularly critical phenomena are represented by LFOs and ULFOs (frequency from 0.01 Hz up to 0.2 Hz), when even very low amplitude disturbances (0.1%) can have detrimental effects on the performance of inductive VTs.

Future works will be focused on the impact of subharmonics on harmonics measurement through inductive CTs and, moreover, the performance of inductive VTs and CTs in subharmonic measurements.

REFERENCES

[1] S. K. Jain and S. N. Singh, "Harmonics estimation in emerging power system: Key issues and challenges," *Electr. Power Syst. Res.*, vol. 81, no. 9, pp. 1754–1766, Sep. 2011.

[2] A. Kalair, N. Abas, A. R. Kalair, Z. Saleem, and N. Khan, "Review of harmonic analysis, modeling and mitigation techniques," *Renew. Sustain. Energy Rev.*, vol. 78, pp. 1152–1187, Oct. 2017.

[3] A. Cataliotti *et al.*, "Compensation of nonlinearity of voltage and current instrument transformers," *IEEE Trans. Instrum. Meas.*, vol. 68, no. 5, pp. 1322–1332, May 2019.

[4] G. Crotti, G. D'Avanzo, D. Giordano, P. S. Letizia, and M. Luiso, "Extended SINDICOMP: Characterizing MV voltage transformers with sine waves," *Energies*, vol. 14, no. 6, p. 1715, Mar. 2021.

[5] A. J. Collin, A. Delle Femine, D. Gallo, R. Langella, and M. Luiso, "Compensation of current transformers' nonlinearities by tensor linearization," *IEEE Trans. Instrum. Meas.*, vol. 68, no. 10, pp. 3841–3849, Oct. 2019.

[6] G. Crotti, D. Giordano, G. D'Avanzo, P. S. Letizia, and M. Luiso, "A new industry-oriented technique for the wideband characterization of voltage transformers," *Measurement*, vol. 182, Sep. 2021, Art. no. 109674.

[7] S. Toscani, M. Faifer, A. Ferrero, C. Laurano, R. Ottoboni, and M. Zanoni, "Compensating nonlinearities in voltage transformers for enhanced harmonic measurements: The simplified volterra approach," *IEEE Trans. Power Del.*, vol. 36, no. 1, pp. 362–370, Feb. 2021.

[8] G. D'Avanzo, A. Delle Femine, D. Gallo, C. Landi, and M. Luiso, "Impact of inductive current transformers on synchrophasor measurement in presence of modulations," *Measurement*, vol. 155, Apr. 2020, Art. no. 107535.

[9] (Aug. 29, 2021). *EMPIR 19NRM05 IT4PQ Project Website*. [Online]. Available: https://www.euramet.org/research-innovation/search-research-projects/details/project/measurement-methods-and-test-procedures-for-assessing-accuracy-of-instrument-transformers-for-power/?L=0&tx_eurametctcp_project%5Baction%5D=show&tx_eurametctcp_project%5Bcontroller%5D=Project&cHash=022ee6ab2e8ea8c12a7ed904625a1cc7

[10] (Aug. 29, 2021). *EMPIR 19NRM05 IT4PQ Project Website*. [Online]. Available: https://www.it4pq.eu/

[11] M. Wu, L. Xie, L. Cheng, and R. Sun, "A study on the impact of wind farm spatial distribution on power system sub-synchronous oscillations," *IEEE Trans. Power Syst.*, vol. 31, no. 3, pp. 2154–2162, May 2016.

[12] Z. Leonowicz, "Power quality in wind power systems," *Renew. Energy Power Qual. J.*, vol. 1, no. 7, pp. 234–238, Apr. 2009.

[13] G. Chen, C. Liu, G. Wang, D. Ai, H. Shi, and Y. Li, "Research on simulation accuracy of ultra-low frequency oscillation in power system with high proportion of hydropower," in *Proc. IEEE 3rd Int. Electr. Energy Conf. (CIEEC)*, Sep. 2019, pp. 834–838.

[14] Q. Liu *et al.*, "Emergency control strategy of ultra-low frequency oscillations based on WAMS," in *Proc. IEEE Innov. Smart Grid Technol. (ISGT Asia)*, May 2019, pp. 296–301.

[15] Y. Chen *et al.*, "Analysis of ultra-low frequency oscillation in Yunnan asynchronous sending system," in *Proc. IEEE Power Energy Soc. Gen. Meeting*, Jul. 2017, pp. 1–5.

[16] N. Jamil, "Low frequency oscillations of hydroelectric power plant," in *Proc. 50th Int. Universities Power Eng. Conf. (UPEC)*, Sep. 2015, pp. 1–6.

[17] R. Langella, A. Testa, S. Z. Djokic, J. Meyer, and E. M. Klatt, "On the interharmonic emission of PV inverters under different operating conditions," in *Proc. 17th Int. Conf. Harmon. Qual. Power (ICHQP)*, Oct. 2016, pp. 733–738.

[18] M. R. Islam, A. M. Mahfuz-Ur-Rahman, K. M. Muttaqi, and D. Sutanto, "State-of-the-art of the medium-voltage power converter technologies for grid integration of solar photovoltaic power plants," *IEEE Trans. Energy Convers.*, vol. 34, no. 1, pp. 372–384, Mar. 2019.

[19] S. Sakar, S. K. Ronnberg, and M. Bollen, "Interharmonic emission in AC–DC converters exposed to nonsynchronized high-frequency voltage above 2 kHz," *IEEE Trans. Power Electron.*, vol. 36, no. 7, pp. 7705–7715, Jul. 2021.

[20] Z. Leonowicz, "Analysis of sub-harmonics in power systems," in *Proc. 9th Int. Conf. Environ. Electr. Eng.*, May 2010, pp. 125–127.

[21] J. Garrido-Zafra, A. Moreno-Munoz, A. R. Gil-de-Castro, F. Bellido-Outeirino, R. Medina-Gracia, and E. Gutierrez-Ballesteros, "Load scheduling strategy to improve power quality in electric-boosted glass furnaces," *IEEE Trans. Ind. Appl.*, vol. 57, no. 1, pp. 953–963, Jan. 2021.

[22] R. F. Chu and J. J. Burns, "Impact of cycloconverter harmonics," *IEEE Trans. Ind. Appl.*, vol. 25, no. 3, pp. 427–435, May 1989.

[23] P. Syam, P. K. Nandi, and A. K. Chattopadhyay, "An improved feedback technique to suppress subharmonics in a naturally commutated cycloconverter," *IEEE Trans. Ind. Electron.*, vol. 45, no. 6, pp. 950–953, Dec. 1998.

[24] P. Syam, G. Bandyopadhyay, P. K. Nandi, and A. K. Chattopadhyay, "Simulation and experimental study of interharmonic performance of a cycloconverter-fedsynchronous motor drive," *IEEE Trans. Energy Convers.*, vol. 19, no. 2, pp. 325–332, Jun. 2004.

[25] F. D. Rosa, R. Langella, A. Sollazzo, and A. Testa, "On the interharmonic components generated by adjustable speed drives," *IEEE Trans. Power Del.*, vol. 20, n. 4, pp. 2535–2543, Oct. 2005.

[26] J. P. G. D. Abreu and A. E. Emanuel, "The need to limit subharmonics injection," in *Proc. 9th Int. Conf. Harmon. Qual. Power.*, vol. 1, Oct. 2000, pp. 251–253.

[27] F. Bonavolonta, L. P. D. Noia, A. Liccardo, S. Tessitore, and D. Lauria, "A PSO-MMA method for the parameters estimation of interarea oscillations in electrical grids," *IEEE Trans. Instrum. Meas.*, vol. 69, no. 11, pp. 8853–8865, Nov. 2020.

[28] A. Testa *et al.*, "Interharmonics: Theory and modeling," *IEEE Trans. Power Del.*, vol. 22, no. 4, pp. 2335–2348, Oct. 2007.

[29] M. Klein, G. J. Rogers, and P. Kundur, "A fundamental study of inter-area oscillations in power systems," *IEEE Trans. Power Syst.*, vol. 6, no. 3, pp. 914–921, Aug. 1991.

[30] J. Barros, M. de Apraiz, and R. I. Diego, "Measurement of subharmonics in power voltages," in *Proc. IEEE Lausanne Power Tech*, Jul. 2007, pp. 1736–1740.

[31] L. Feola, R. Langella, and A. Testa, "On the effects of unbalances, harmonics and interharmonics on PLL systems," *IEEE Trans. Instrum. Meas.*, vol. 62, no. 9, pp. 2399–2409, Sep. 2013.

[32] J. Matas, M. Castilla, J. Miret, L. G. de Vicuna, and R. Guzman, "An adaptive prefiltering method to improve the speed/accuracy tradeoff of voltage sequence detection methods under adverse grid conditions," *IEEE Trans. Ind. Electron.*, vol. 61, no. 5, pp. 2139–2151, May 2014.

[33] R. Langella, A. Testa, and A. E. Emanuel, "On the effects of subsynchronous interharmonic voltages on power transformers: Single phase units," *IEEE Trans. Power Del.*, vol. 23, n. 4, pp. 2480–2487, Oct. 2008.

[34] *IEEE Recommended Practice and Requirements for Harmonic Control in Electric Power Systems—Redline*, Standard 519-2014 IEEE, Jun. 2014, pp. 1–213.

[35] *IEEE Recommended Practice for Monitoring Electric Power Quality*, Standard 1159, IEEE, 2019.

[36] *Electromagnetic Compatibility (EMC)—Part 2-12: Environment—Compatibility Levels for Low-Frequency Conducted Disturbances and Signalling in Public Medium-Voltage Power Supply systems*, Standard IEC 61000-2-12, IEC, 2003.

[37] *Electromagnetic Compatibility (EMC)—Part 3-6: Limits—Assessment of Emission Limits for the Connection of Distorting Installations to MV, HV and EHV Power Systems*, Standard IEC TR 61000-3-6:2008, IEC, 2008.

[38] *Electromagnetic Compatibility (EMC)—Part 2-4: Environment—Compatibility Levels in Industrial Plants for Low-Frequency Conducted Disturbances*, Standard IEC 61000-2-4, IEC, 2002.

[39] P. Kinsler, "Faraday's law and magnetic induction: Cause and effect, experiment and theory," *Physics*, vol. 2, no. 2, pp. 148–161, May 2020.

[40] IEC 60050—International Electrotechnical Vocabulary—Details for IEV number 411-47-02. (Aug. 29, 2021). *Magnetization Characteristic*. [Online]. Available: https://www.electropedia.org/iev/iev.nsf/display?openform&ievref=411-47-02

[41] *Electromagnetic Compatibility (EMC)—Part 4-30: Testing and Measurement Techniques—Power Quality Measurement Methods*, Standard IEC 61000-4-30, IEC, 2015.

[42] A. J. Collin, A. Delle Femine, C. Landi, R. Langella, M. Luiso, and A. Testa, "The role of supply conditions on the measurement of high-frequency emissions," *IEEE Trans. Instrum. Meas.*, vol. 69, no. 9, pp. 6667–6676, Sep. 2020.

[43] G. Crotti *et al.*, "Frequency compliance of MV voltage sensors for smart grid application," *IEEE Sensors J.*, vol. 17, no. 23, pp. 7621–7629, Dec. 2017.

[44] M. Zucca, M. Modarres, D. Giordano, and G. Crotti, "Accurate numerical modelling of MV and HV resistive dividers," *IEEE Trans. Power Del.*, vol. 32, no. 3, pp. 1645–1652, Jun. 2017.

[45] *Instrument Transformers—Part 3: Additional Requirements for Inductive Voltage Transformer*, Standard IEC 61869-3, IEC, 2011.

Gabriella Crotti received the Laurea degree (*cum laude)* in physics from the University of Torino, Turin, Italy, in 1986.

Since then she has been with the Istituto Nazionale di Ricerca. Metrologica (INRIM) of Torino, Turin, where she presently works as a Director Technologist in the electric and electromagnetic field and system sector. Her research interests are focused on the development and characterization of references and techniques for voltage and current measurements in high and medium voltage grids and on the traceability of electric and magnetic field measurements at low and intermediate-frequency. She is presently leading the EMPIR project 19NRM05 IT4PQ.

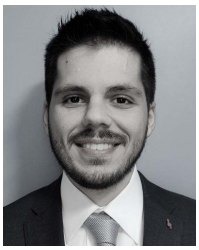

Giovanni D'Avanzo was born in Naples, Italy, in 1991. He received the M.Sc. degree (*summa cum laude*) in electronic engineering from the University of Campania Luigi Vanvitelli, Aversa (CE), Italy, in 2019, where he is currently pursuing the Ph.D. degree in energy conversion.

He is working on various European metrology research projects. His research interests include the characterization of Instrument Transformers under power quality phenomena, the development of smart meters, and measurement systems for e-vehicles.

Palma Sara Letizia was born in Caserta, Italy, in 1992. She received the M.Sc. degree (*summa cum laude*) in power electronic engineering from the University of Campania Luigi Vanvitelli, Aversa (CE), Italy, in 2018. She is currently pursuing the Ph.D. degree in metrology with the Politecnico di Torino and Istituto Nazionale di Ricerca Metrologica (INRIM), Turin, Italy.

Her main scientific interest is metrology applied to power grids. In particular, the development of new procedures and reference sensors for power quality and phasor measurement unit applications and the definition of traceable characterization methods for medium voltage transducers under nonsinusoidal conditions.

Mario Luiso (Member, IEEE) was born in Naples, Italy, on July 6, 1981. He received the Laurea degree in electronic engineering (*summa cum laude*) and the Ph.D. degree in electrical energy conversion from the University of Campania Luigi Vanvitelli, Aversa (CE), Italy, in 2005 and 2007, respectively.

He currently is an Associate Professor with the Department of Engineering, University of Campania Luigi Vanvitelli. His main scientific interests are related to the development of innovative methods, sensors, and instrumentation for power system measurements, in particular, power quality, calibration of instrument transformers, phasor measurement units, and smart meters. He is the author and coauthor of more than 200 articles published in books, scientific journals, and conference proceedings.

Dr. Luiso is a member of the IEEE Instrumentation and Measurement Society.